

Supplemental Text

Transcriptional regulation of *Caenorhabditis elegans* FOXO/DAF-16 modulates lifespan

Ankita Bansal, Eun-Soo Kwon, Darryl Conte Jr , Haibo Liu, Michael J. Gilchrist, Lesley T.

MacNeil, and Heidi A. Tissenbaum

Supplementary Data

***daf-16d/f* is the most abundant *daf-16* isoform in adult worms**

We find that *daf-16* is regulated at the level of transcription as worms age. To systematically analyze the comparative level of each *daf-16* isoform in the early adult stage, we designed isoform-specific primers as well as primers covering 3' sequences shared by each isoform (Table S7). Isoform-specific primers were specific to their respective target (data not shown). Since it is possible that the different *daf-16* primer sets could show different amplification efficiency, we first measured the *daf-16* mRNA level of *daf-16* isoform transgenic worms using isoform-specific primers as well as isoform-common primers (Figure S8A, B). Since these worms express the isoform specific transgene, the Ct values should be the same between the common and isoform specific values. However, we found that the isoform-specific primers and isoform-common primers produce different Ct values, Ct_{iso} vs Ct_{com} respectively, and this was most apparent for *daf-16b* (Figure S8-S9). Therefore, to directly compare the levels between the different *daf-16* isoforms, we calculated the ΔCt by subtracting the Ct_{com} value from the Ct_{iso} value (S10C). This is the $\Delta Ct_{calibration}$ (ΔCt_{S8}) shown in Figure S9. Importantly, for each *daf-16* isoform, the two biological repeats provided similar $\Delta Ct_{calibration}$ (ΔCt_{S8}) ($Ct_{iso} - Ct_{com}$) values (Figure S8C).

To compare the level of each *daf-16* isoform in day 1 adult *daf-2(e1370)* mutants, we first measured Ct value for each *daf-16* isoform using isoform-specific primers (Figure S9A); $Ct_{iso}^{daf-16a}$, $Ct_{iso}^{daf-16b}$, $Ct_{iso}^{daf-16d/f}$. Then, using the common primers, we measured the Ct value to obtain the $Ct_{com}^{daf-16\ total}$. The ΔCt for each isoform was determined by $Ct_{isoform} - Ct_{endogenous\ control}$ (Figure S9). Then to determine the $\Delta\Delta Ct$, we took the $\Delta Ct_{isoform} - \Delta Ct_{calibrator}$ (from S8) as shown in Figure S9. To determine the relative abundance of each *daf-16* isoform in day 1 adult *daf-2* mutants, we calculated $2^{-\Delta\Delta Ct}$ (Figure S9). Importantly, the sum of the relative levels of each *daf-16* isoform was around 1 (Figure S9B). Last, in two independent sample repeats, *daf-16d/f* was found to comprise more than 80 % of total *daf-16*, suggesting DAF-16d/f is the major isoform in early adult worms (Figure S9C).

Supplementary Figures:

Figure S1. Comparative DAF-16 protein levels in different *daf-16a* transgenic worm strains.

Equal amounts of lysates prepared from approximately 100 worms were loaded onto 10%SDS PAGE gel, and immunoblotted with anti- α -DAF-16 and anti- α -tubulin. See Methods for additional details.

Figure S2. Effect of dosage of transgene on the spatial distribution of DAF-16a

Nuclear/cytosolic distribution of DAF-16a in four *daf-16(mgDf50); daf-2(e1370); daf-16a* transgenic worms grown at 15°C. The nuclear/cytosolic ratio of DAF-16a::GFP was measured using Image J software. The mean ratio is plotted and the error bars represent the Standard Deviation. Two independent repeats are shown.

Figure S3. High doses of *daf-16a* transgene is toxic to worm

Comparison of the growth rates of different *daf-16a::gfp* transgenic strains in *daf-16(mgDf50)* background and *daf-16(mgDf50); daf-2(e1370)*.

Figure S4. *daf-16a* and *daf-16d/f* regulate lifespan differently in response to levels of IIS knockdown

Lifespan analysis of *daf-16a* and *daf-16d/f* transgenes in either in *daf-2(e1370)*, and *daf-2(e1368)* genetic background. Bar graphs represent an average of the mean lifespan with the Standard Deviation for three independent experiments. All lifespan data are summarized in Table S3 and Table S4.

Figure S5. *daf-16a* and *daf-16d/f* regulate dauer development differently in response to levels of IIS knockdown

Dauer formation of *daf-16(mgDf50)*; *daf-16* isoform transgenic worms in either a *daf-2(e1370)* or a *daf-2(e1368)* mutant background at 20°C and 25°C. (A) Repeat 1; At 20°C, mean dauer formation is as follows: *daf-2(e1370)*, 90.9 ± 5.5 % (n=440); *daf-16(mgDf50)*; *daf-2(e1370)*, 0 % (n>300); *daf-16(mgDf50)*; *daf-2(e1370)*; *daf-16a*, 2.8 ± 1.4 % (n=787); *daf-16(mgDf50)*; *daf-2(e1370)*; *daf-16d/f*, 63.4 ± 2.4 % (n=719); *daf-2(e1368)*, 1.4 ± 0.2 % (n=785); *daf-16(mgDf50)*; *daf-2(e1368)*, 0 % (n>300); *daf-16(mgDf50)*; *daf-2(e1368)*; *daf-16a*, 0.4 ± 0.0 % (n=775); *daf-16(mgDf50)*; *daf-2(e1368)*; *daf-16d/f*, 0 % (n=768). At 25°C, mean dauer formation is as follows: *daf-2(e1370)*, 100 % (n=498); *daf-16(mgDf50)*; *daf-2(e1370)*, 0 % (n>300); *daf-16(mgDf50)*; *daf-2(e1370)*; *daf-16a*, 100 % (n=679); *daf-16(mgDf50)*; *daf-2(e1370)*; *daf-16d/f*, 100 % (n=662); *daf-2(e1368)*, 100 % (n=613); *daf-16(mgDf50)*; *daf-2(e1368)*, 0 % (n>205); *daf-16(mgDf50)*; *daf-2(e1368)*; *daf-16a*, 97.9 ± 1.6 % (n=786); *daf-16(mgDf50)*; *daf-2(e1368)*; *daf-16d/f*, 38.9 ± 7.6 % (n=682). (B) Repeat 2; At 20°C, mean dauer formation is as follows: *daf-2(e1370)*, 98.5 ± 0.6 % (n=405); *daf-16(mgDf50)*; *daf-2(e1370)*, 0 % (n=532); *daf-16(mgDf50)*; *daf-2(e1370)*; *daf-16a*, 13.9 ± 5.0 % (n=517); *daf-16(mgDf50)*; *daf-2(e1370)*; *daf-16d/f*, 64.2 ± 8.5 % (n=595); *daf-2(e1368)*, 8.8 ± 1.9 % (n=524); *daf-16(mgDf50)*; *daf-2(e1368)*, 0 % (n=542); *daf-16(mgDf50)*; *daf-2(e1368)*; *daf-16a*, 2.6 ± 1.2 % (n=622); *daf-16(mgDf50)*; *daf-2(e1368)*; *daf-16d/f*, 0 % (n=554). At 25°C, mean dauer formation is as follows: *daf-2(e1370)*, 100 % (n=248); *daf-16(mgDf50)*; *daf-2(e1370)*, 0 % (n>300); *daf-16(mgDf50)*; *daf-2(e1370)*; *daf-16a*, 100 % (n=548); *daf-16(mgDf50)*; *daf-2(e1370)*; *daf-16d/f*, 100 % (n=535); *daf-2(e1368)*, 100 % (n=402); *daf-16(mgDf50)*; *daf-2(e1368)*, 0 % (n=205); *daf-16(mgDf50)*; *daf-2(e1368)*; *daf-16a*, 100 % (n=569); *daf-16(mgDf50)*; *daf-2(e1368)*; *daf-16d/f*, 80.2 ± 1.7 % (n=465).

Figure S6. Upregulation of *daf-16d/f* levels as the worms age

Temporal expression pattern of *daf-16d/f*. GFP become brighter with age in *daf-16(mgDf50); daf-2(e1370); daf-16d/f::gfp* transgenic worms. Worms were grown at 15°C and L2, L4, and day 2 worms were visualized with a 1 sec exposure time.

Figure S7. Endogenous transcript levels of *daf-16d/f* is upregulated with age

The expression profiles of three *daf-16* isoforms in wild type N2 (A, C) and long-lived *daf-2(e1370)* strains (B, D). The mRNA levels of *daf-16a*, *daf-16b*, *daf-16d/f* were determined using Quantitative-RT PCR analysis. In both repeats, the expression of *daf-16d/f* is upregulated, compared to *daf-16a* and *daf-16b*. The primer sequences are listed in Table S7.

Figure S8. Quantitative-RT PCR showing differential amplification efficiency with different primers.

(A, B) The mRNA levels of the *daf-16* isoforms in *daf-16(mgDf50); daf-2(e1370); daf-16 isoform* transgenic strains were measured using isoform specific primers and isoform common primers. (C) Respective Ct values (Ct_{iso} , and Ct_{com}) were calculated with threshold of 0.2. Two biological repeats provide similar ΔCt values ($Ct_{iso} - Ct_{com}$); $\Delta Ct^{daf-16a}$, 1.28 ± 0.06 ; $\Delta Ct^{daf-16b}$, 3.70 ± 0.29 ; $\Delta Ct^{daf-16d/f}$, 0.68 ± 0.04 . $\Delta Ct_{calibration}$ values were used in the analysis of the relative abundance of each isoform in the transcriptional analysis of *daf-2(e1370)* in Figure S11.

Figure S9. *daf-16d/f* is the most abundant transcript in day 1 adult *daf-2(e1370)* worms.

(A) The mRNA levels of three *daf-16* isoforms of *daf-2(e1370)* worms were measured using isoform specific primers and isoform common primers. (B) The respective Ct values ($Ct_{iso}^{daf-16a}$, $Ct_{iso}^{daf-16b}$, $Ct_{iso}^{daf-16d/f}$, and $Ct_{com}^{daf-16total}$) were calculated with a threshold of 0.2. (C) Comparative mRNA levels of different *daf-16* isoforms. See Supplementary Text for Experimental Details.

Figure S10. Temporal *daf-16* RNAi treatment to *daf-16(mgDf50); daf-2(e1370); daf-16f::gfp* transgenic worms.

Transgenic worms were grown on HT115 bacterial food. L4 staged worms were transferred to serially diluted *daf-16* RNAi plates containing FUDR; (A) control food, (B) *daf-16* RNAi food, (C) 1/4 diluted *daf-16* RNAi food, (D) 1/16 diluted *daf-16* RNAi food, (E) 1/64 diluted *daf-16* RNAi food. After two days on RNAi plates, worms were moved back to control food. Pictures were taken at both 10X and 40X magnification as shown in the figure. Worms were visualized at indicated time points with 500mS exposure time. The 1/4 and 1/16 dilutions maintained the GFP levels of day-2 old worms similar to L4 stages and were used for lifespan analysis.

Figure S11. Effect of *elt-2* and *swn-1* RNAi on *Pdaf-16a::gfp* expression.

Pdaf-16a::gfp strains were grown on RNAi of *elt-2* or *swn-1*. L4 stage or day 2 adult worms were visualized. The anterior part of the intestine was marked with a dotted line.

Figure S12. Transcription factors regulate the expression of *daf-16a* and *daf-16d/f*.

The temporal expression profiles of *daf-16a* and *daf-16d/f* in wild type or *daf-2(e1370)* strains when (A) *elt-2* or (B) *swn-1* were knocked-down. The mRNA levels of *daf-16a* and *daf-16d/f* were determined using Quantitative-RT PCR analysis. In two biological repeats, the temporal upregulation of *daf-16d/f* is significantly reduced compared to control.

Figure S13. Effect by RNAi of GATA transcription factors on *Pdaf-16d/f::gfp* expression.

(A) Visualization of L4 stage *Pdaf-16d/f::gfp* transgenic worms. (B) Visualization of Day 2 adult *Pdaf-16d/f::gfp* worms. Worms are grown on the indicated RNAi bacteria from hatching.

Figure S14. Effect by RNAi of SWI/SNF complex components on *Pdaf-16d/f::gfp* expression.

(A) Visualization of L4 stage *Pdaf-16d/f::gfp* transgenic worms. (B) Visualization of Day 2 adult *Pdaf-16d/f::gfp* worms. Worms are grown on indicated RNAi bacteria from hatching.

Figure S15: Lack of an effect of FuDR on lifespan.

The strains show similar lifespan curves without FuDR. A concentration of 400uM FuDR was used.

Supplementary Tables:

Table S1- Analysis of the ESTs that correspond to *daf-16*

Table S2- Comparison of levels of *daf-16* isoform transcript

Table S3- Lifespan analysis of *daf-16* isoform transgenic strains

Table S4- Lifespan analysis of *daf-16* isoform transgenic strains

Table S5- Lifespan analysis of serially diluted *daf-16* RNAi

Table S6- Lifespan analysis of GATA transcription factors and SWI/SNF components

Table S7- List of Primers used in this study

Table S8- List of Strains used in this study

Figure S1. Comparative DAF-16 protein levels in different *daf-16a* transgenic worm strains

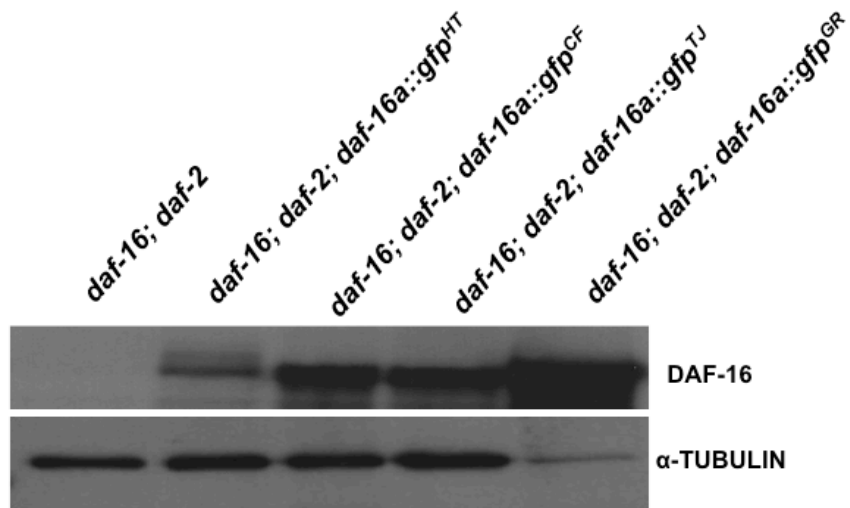


Figure S2. Effect of dosage of transgene on the spatial distribution of DAF-16a

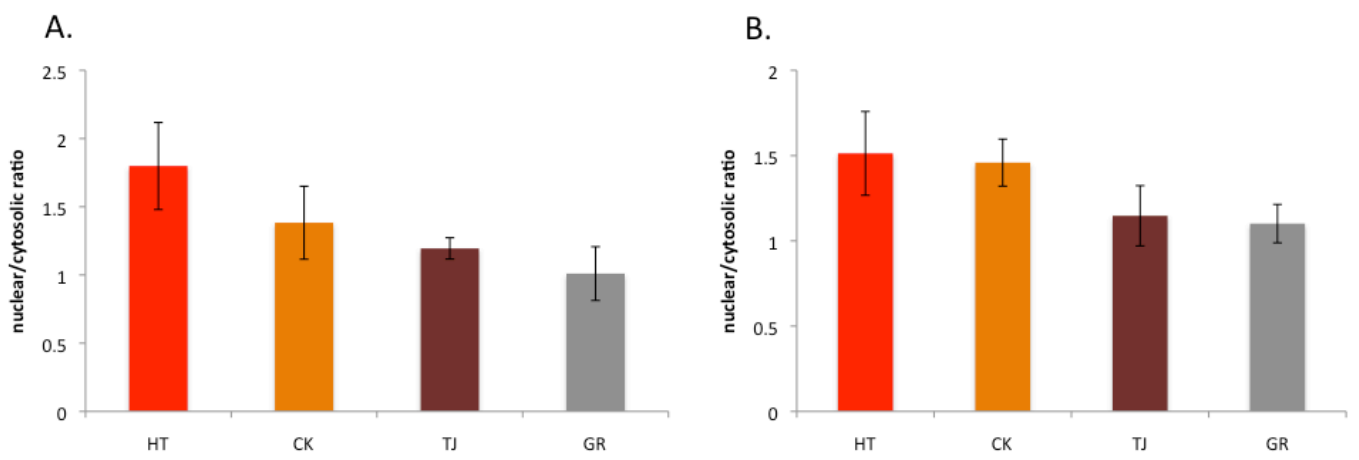


Figure S3. High doses of *daf-16a* transgene is toxic to worm

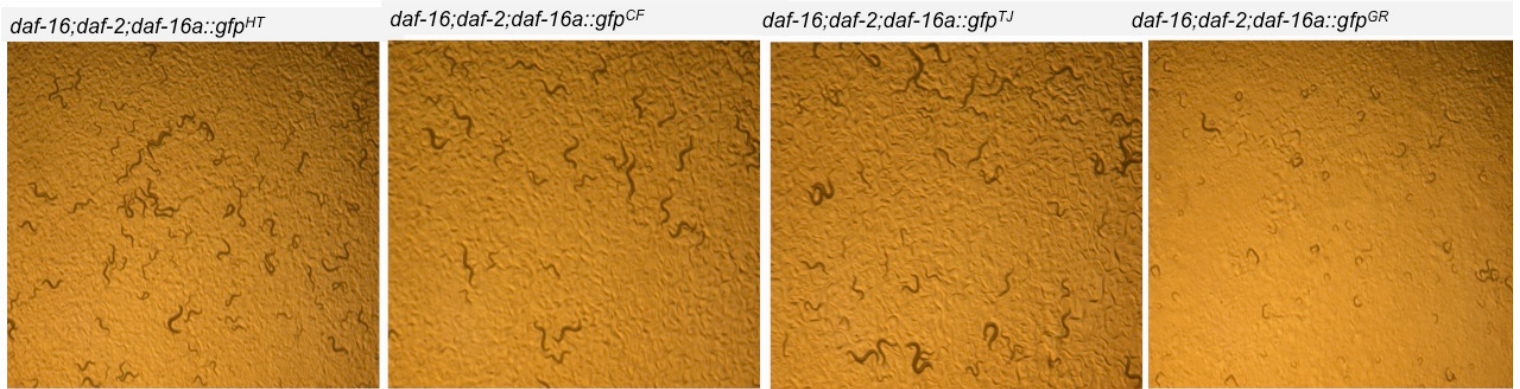


Figure S4. *daf-16a* and *daf-16d/f* regulate lifespan differently in response to levels of IIS knockdown

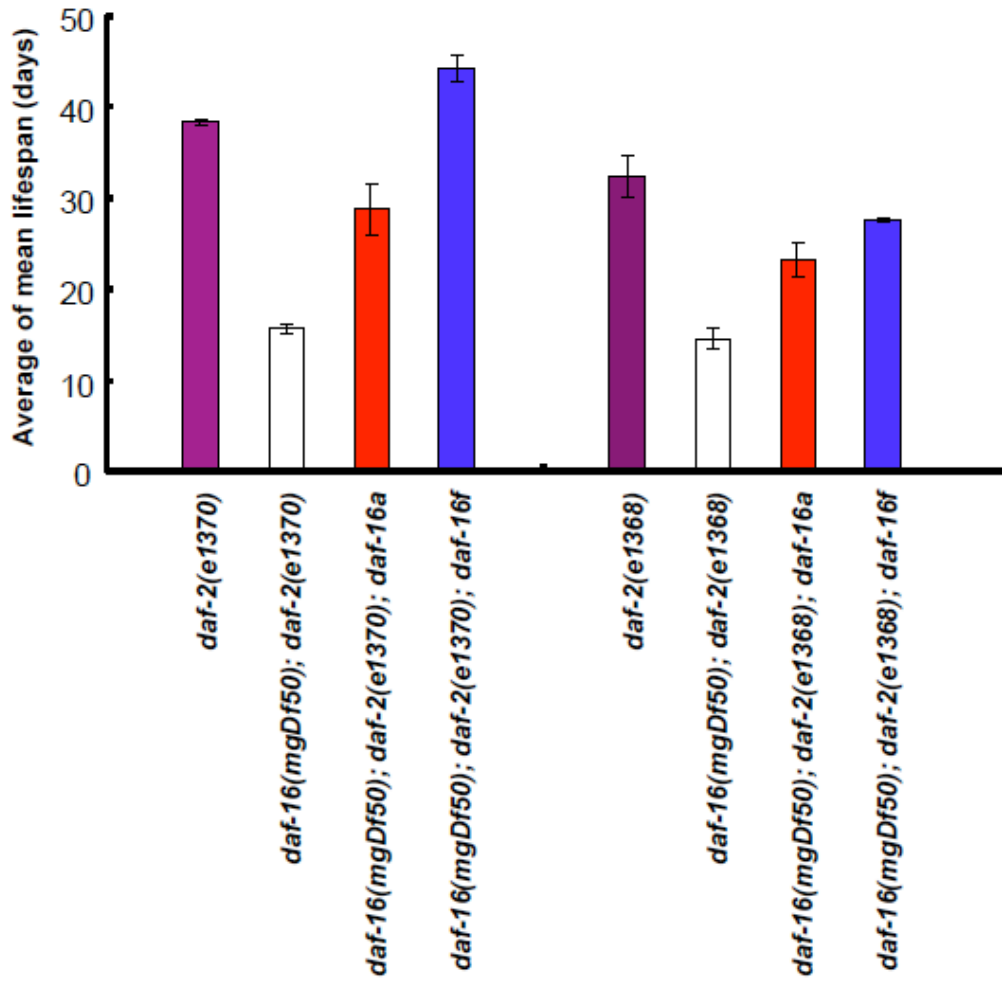
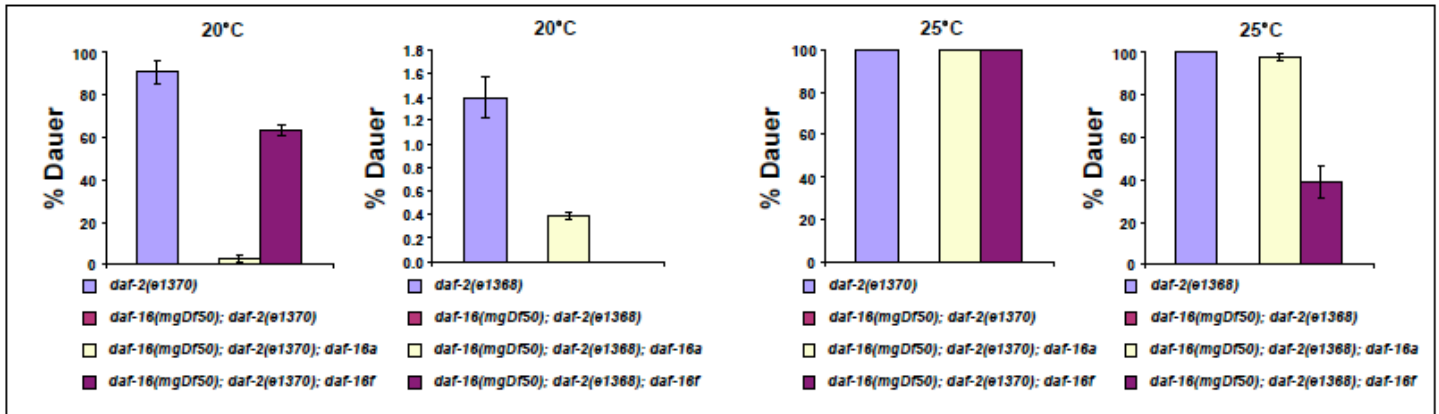


Figure S5. *daf-16a* and *daf-16d/f* regulate dauer development differently in response to levels of IIS knockdown

A



B

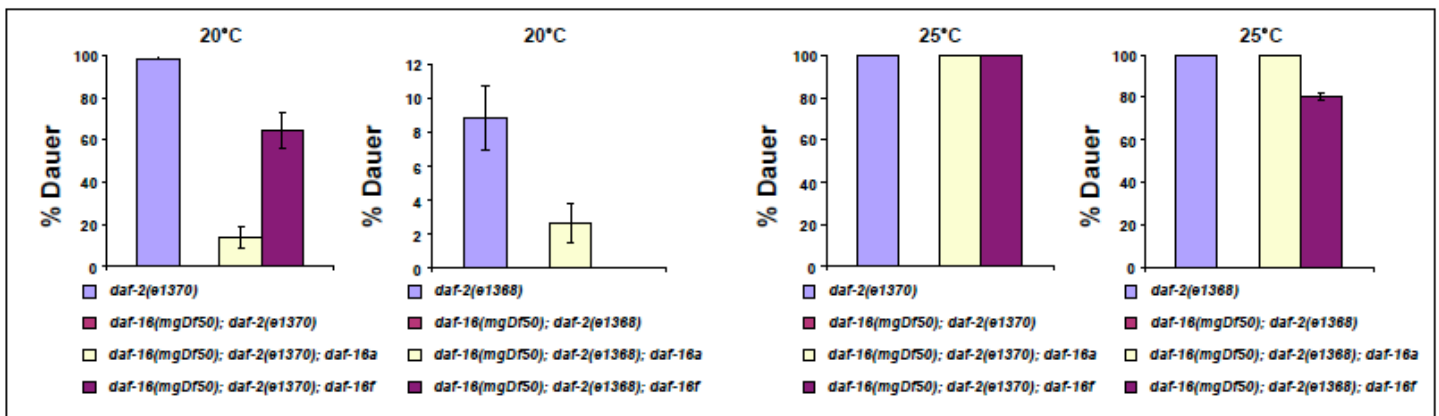


Figure S6. Upregulation of *daf-16d/f* levels as the worms age

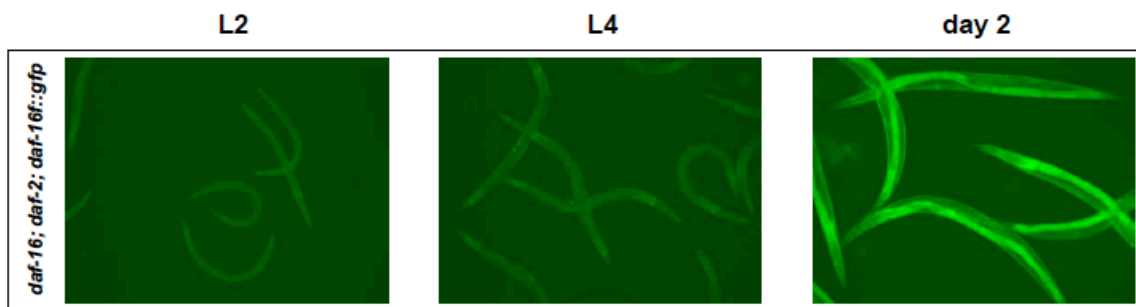


Figure S7. Endogenous transcript levels of *daf-16d/f* is upregulated with age

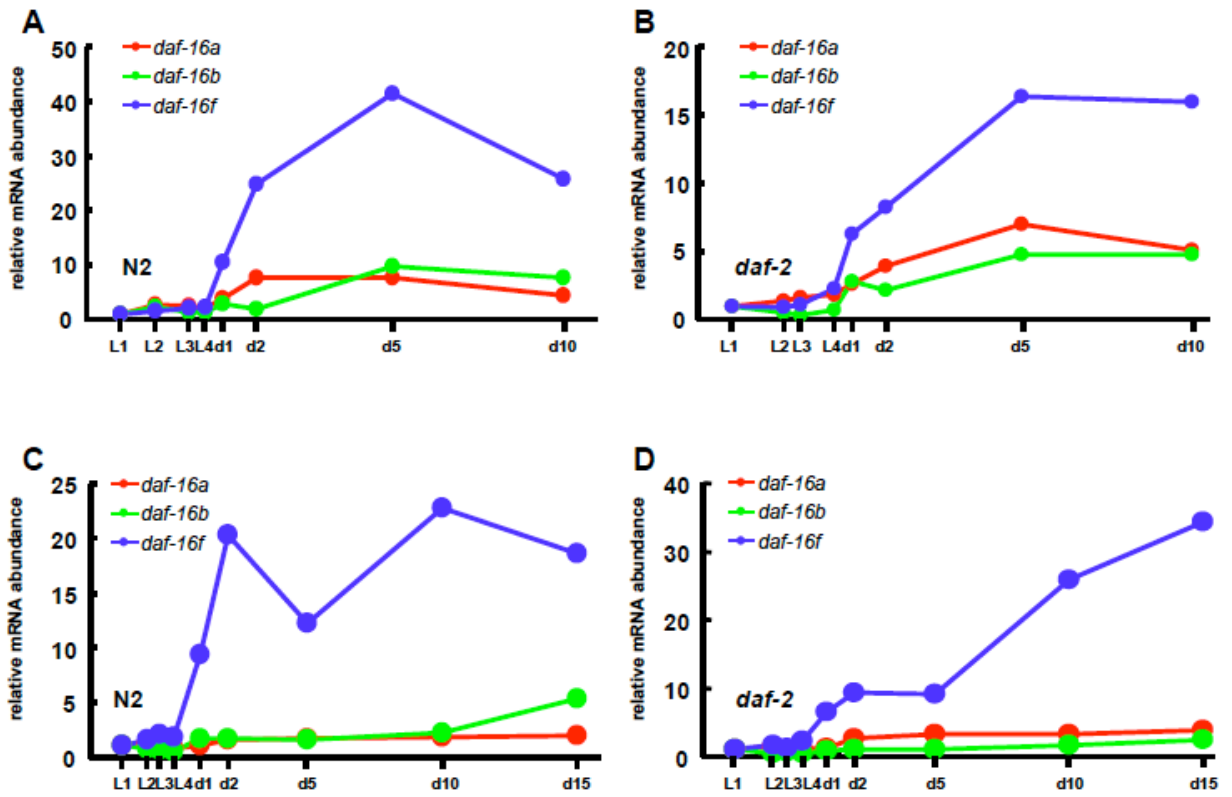


Figure S8. Quantitative-RT PCR showing differential amplification efficiency with different primers.

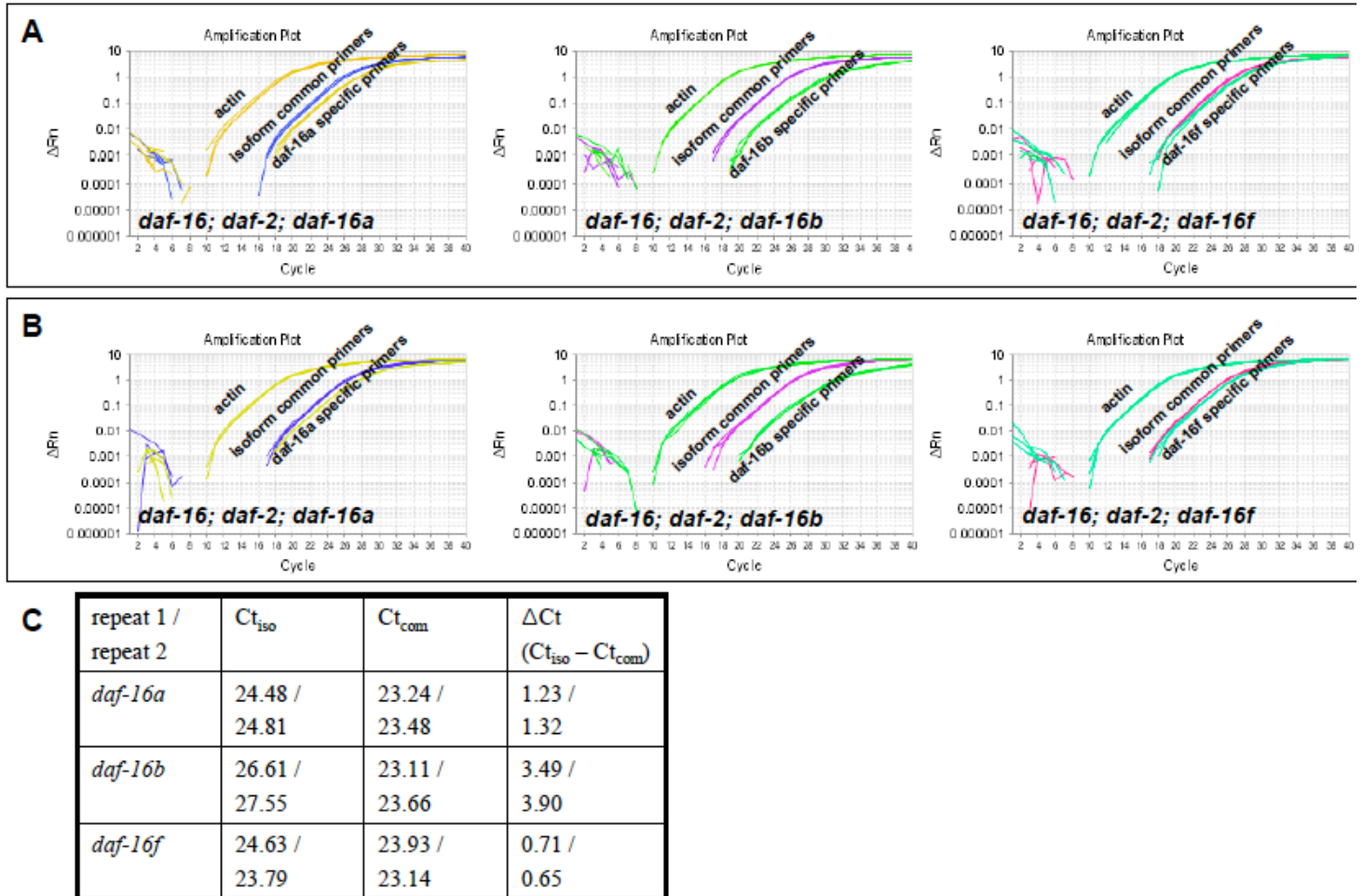
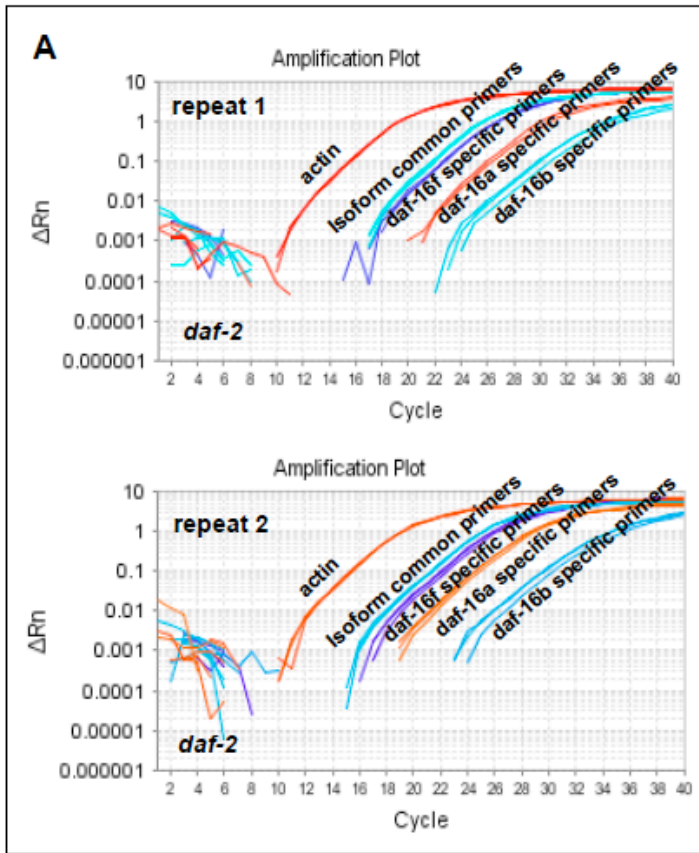


Figure S9. *daf-16d/f* is the most abundant transcript in day 1 adult *daf-2(e1370)* worms.



B

repeat 1	Ct_{iso}	Ct_{com}^{**} ($Ct_{iso} - \Delta Ct^*$)	$Ct_{com}^{**} -$ $Ct_{com}^{daf-16total}$	Relative abundance
<i>daf-16a</i>	27.30	26.06	3.21	0.11
<i>daf-16b</i>	31.11	27.62	4.76	0.04
<i>daf-16f</i>	23.76	23.06	0.20	0.87
<i>daf-16total</i>	N/A	22.86	0.00	1 (1.02)
repeat 2	Ct_{iso}	Ct_{com}^{**} ($Ct_{iso} - \Delta Ct^*$)	$Ct_{com}^{**} -$ $Ct_{com}^{daf-16total}$	Relative abundance
<i>daf-16a</i>	25.79	24.46	2.09	0.23
<i>daf-16b</i>	30.91	27.01	4.64	0.04
<i>daf-16f</i>	23.22	22.57	0.20	0.87
<i>daf-16total</i>	N/A	22.37	0.00	1 (1.14)

Figure S10A. *daf-16(mgDf50); daf-2(e1370); daf-16f::gfp* transgenic worms grown on control food (vector RNAi)

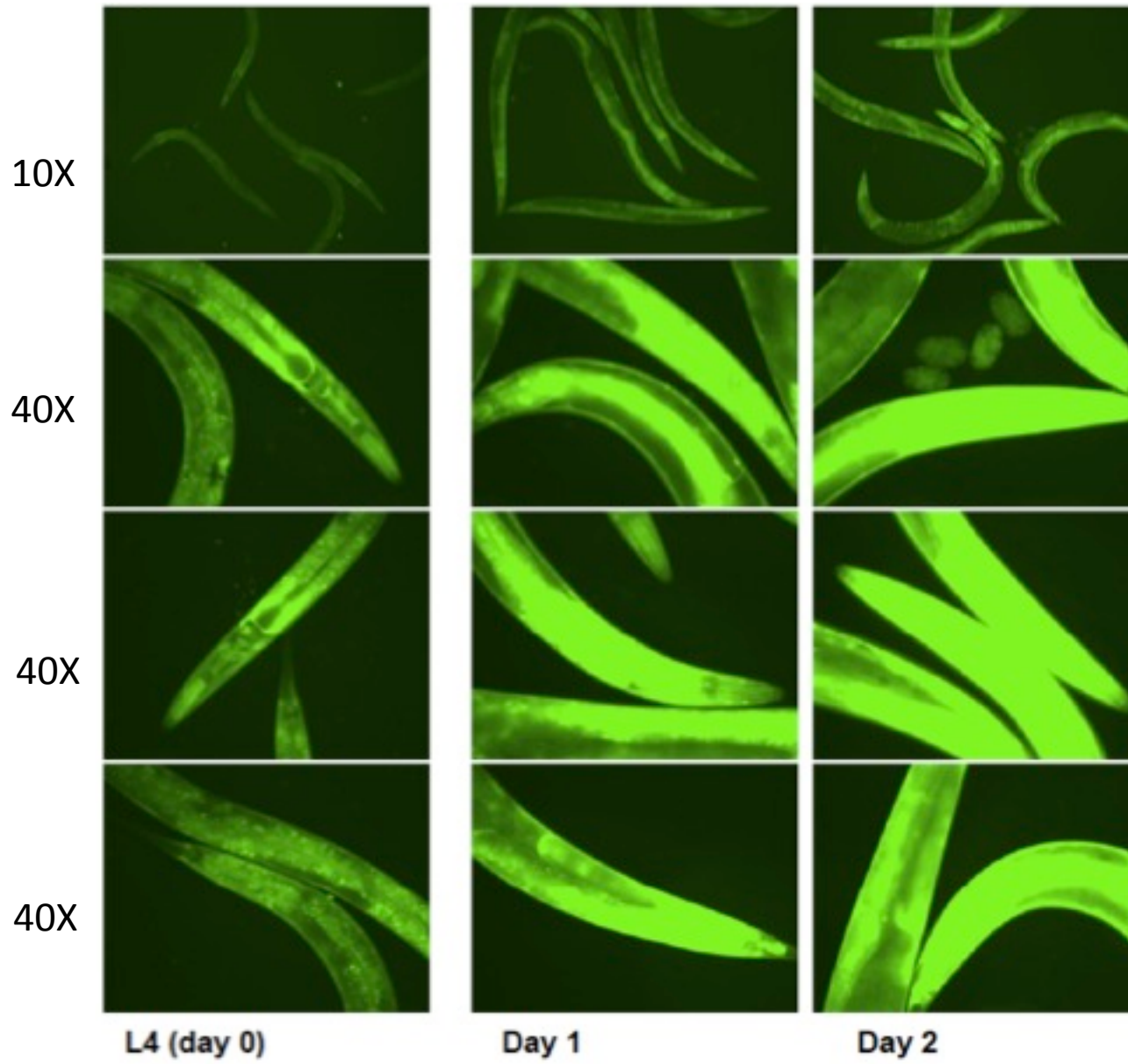


Figure S10B-*daf-16(mgDf50); daf-2(e1370); daf-16f::gfp* transgenic worms grown on *daf-16* RNAi food

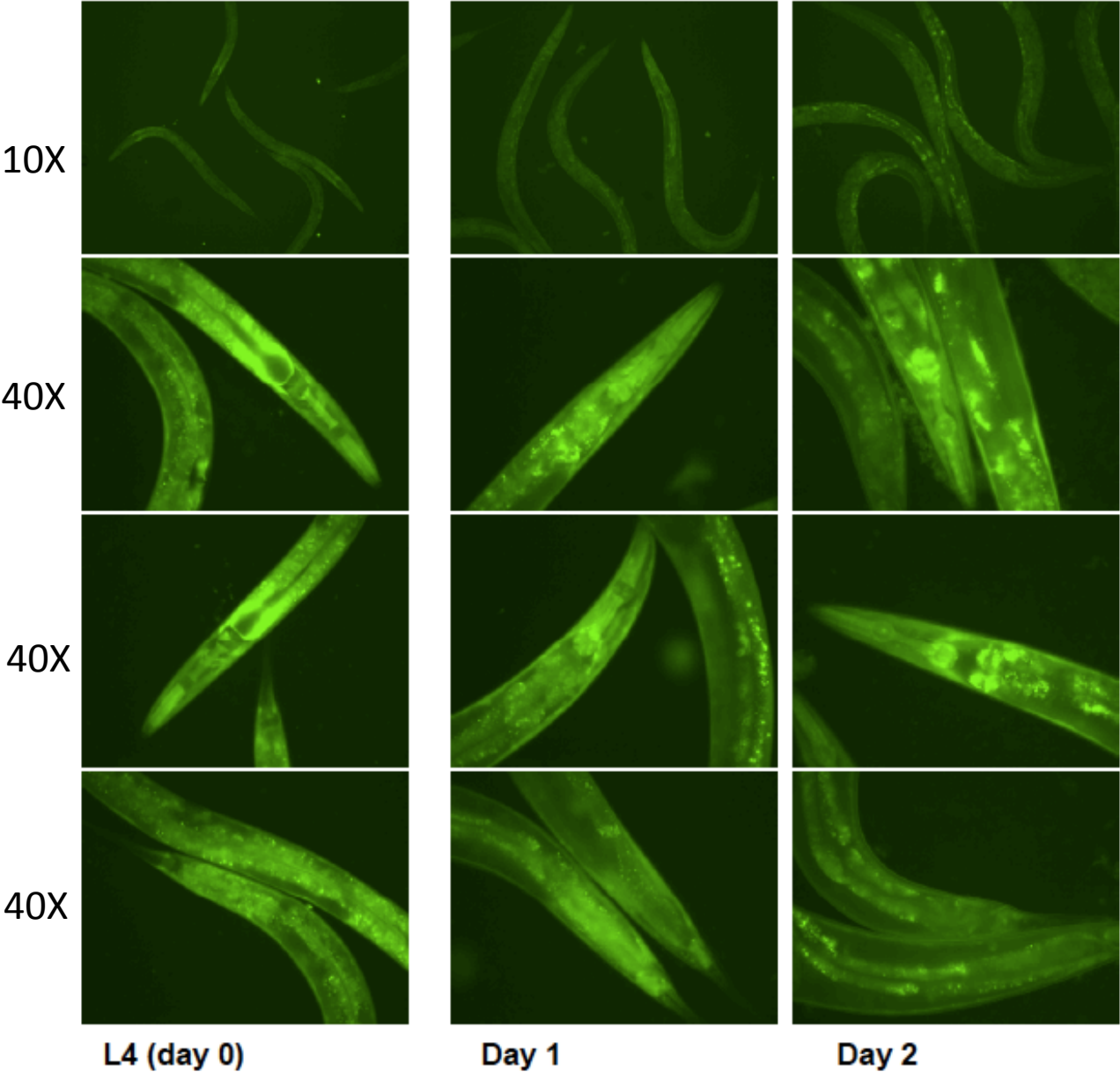


Figure S10C. *daf-16(mgDf50); daf-2(e1370); daf-16f::gfp* transgenic worms grown on 1/4 diluted *daf-16* RNAi food

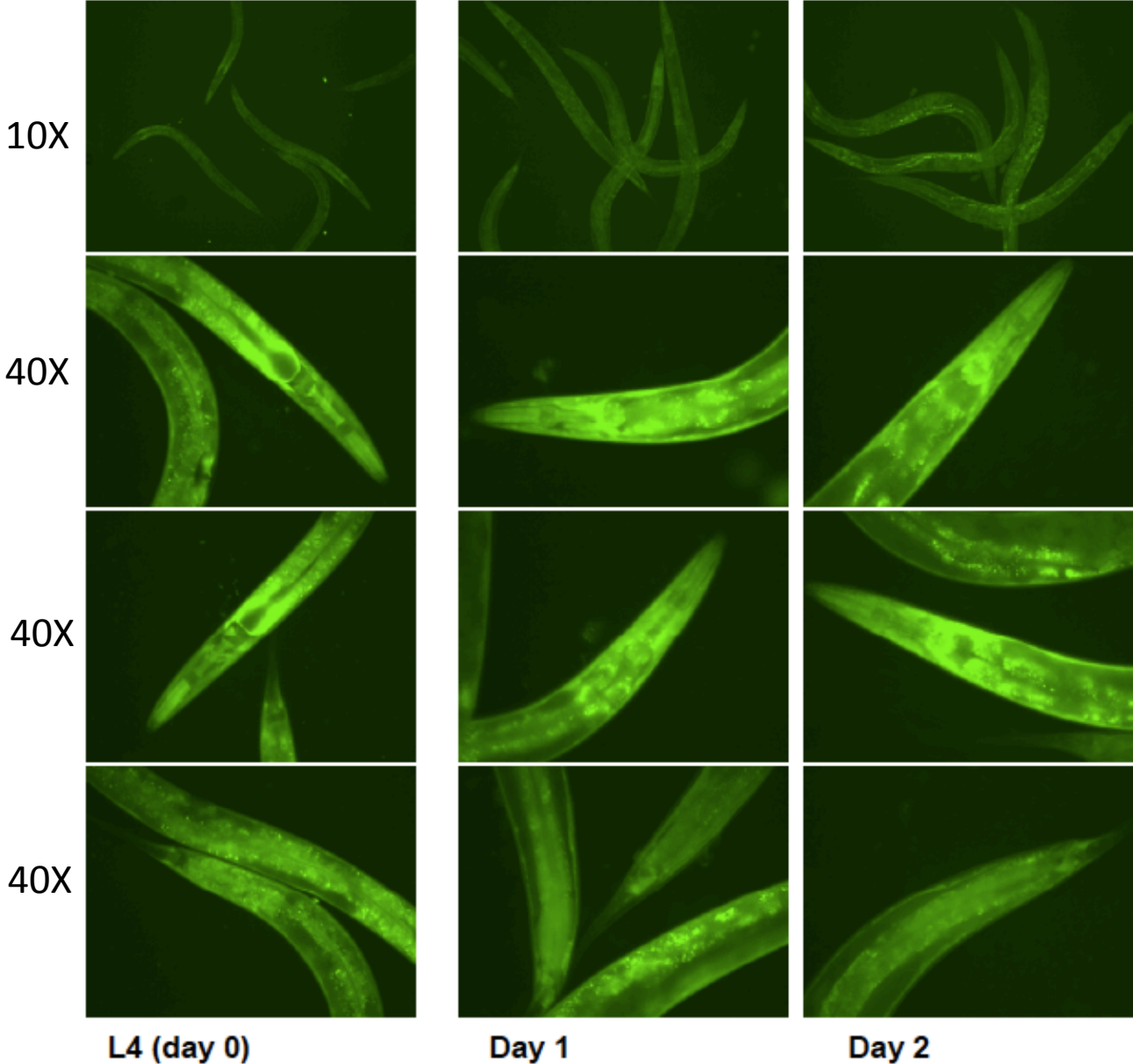


Figure S10D. *daf-16(mgDf50); daf-2(e1370); daf-16f::gfp* transgenic worms grown on 1/16 diluted *daf-16* RNAi food

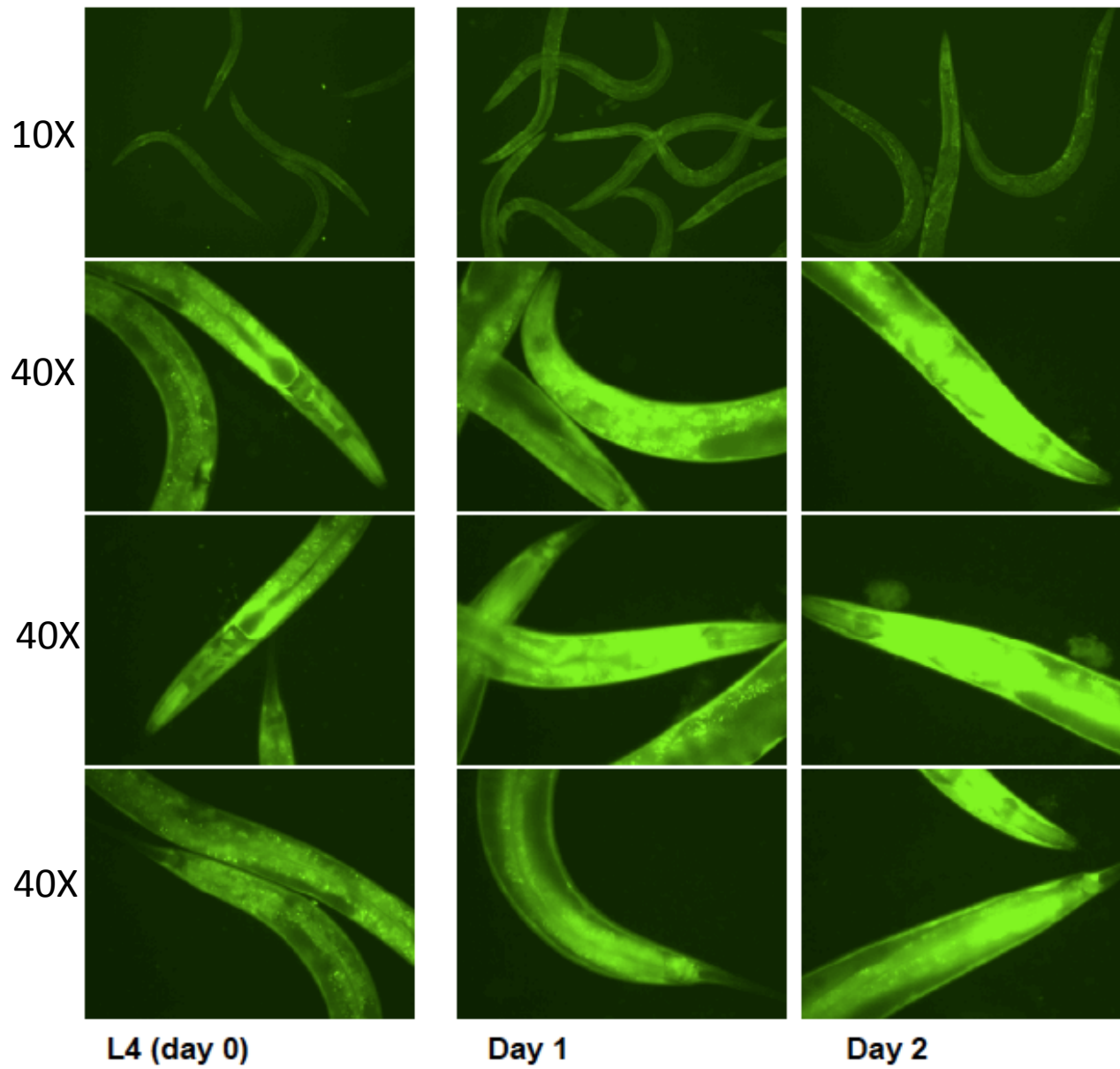


Figure S10E. *daf-16(mgDf50); daf-2(e1370); daf-16::gfp* transgenic worms grown on 1/64 diluted *daf-16* RNAi food

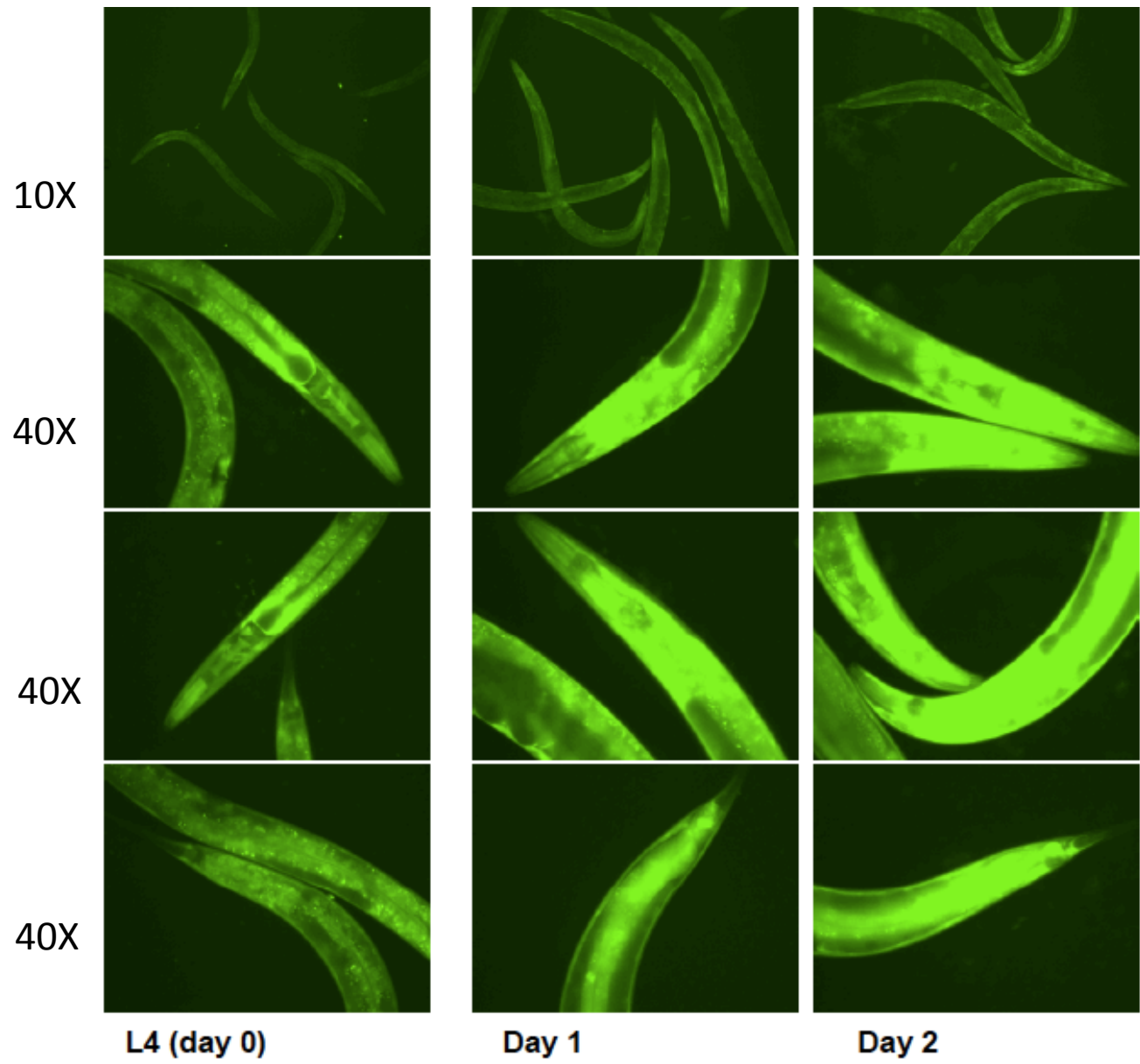


Figure S11. Effect of *elt-2* and *swn-1* RNAi on *Pdaf-16a::gfp* expression.

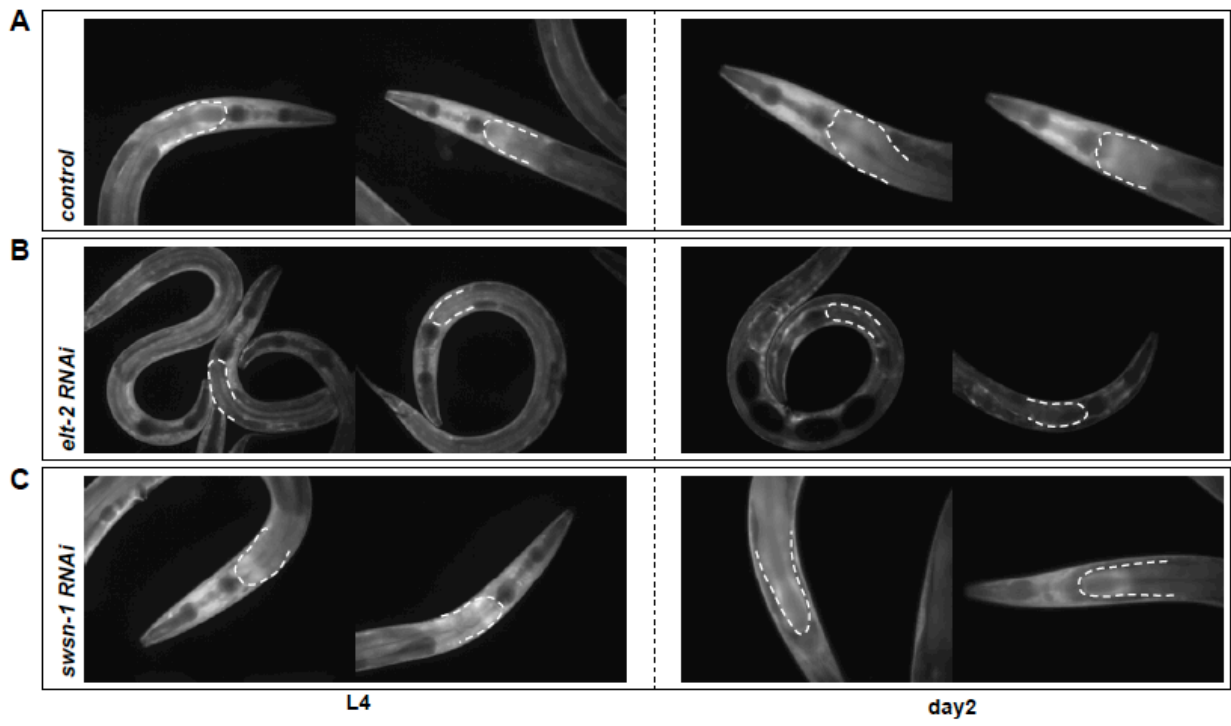


Figure S13. Effect by RNAi of GATA transcription factors on *Pdaf-16d/f::gfp* expression.

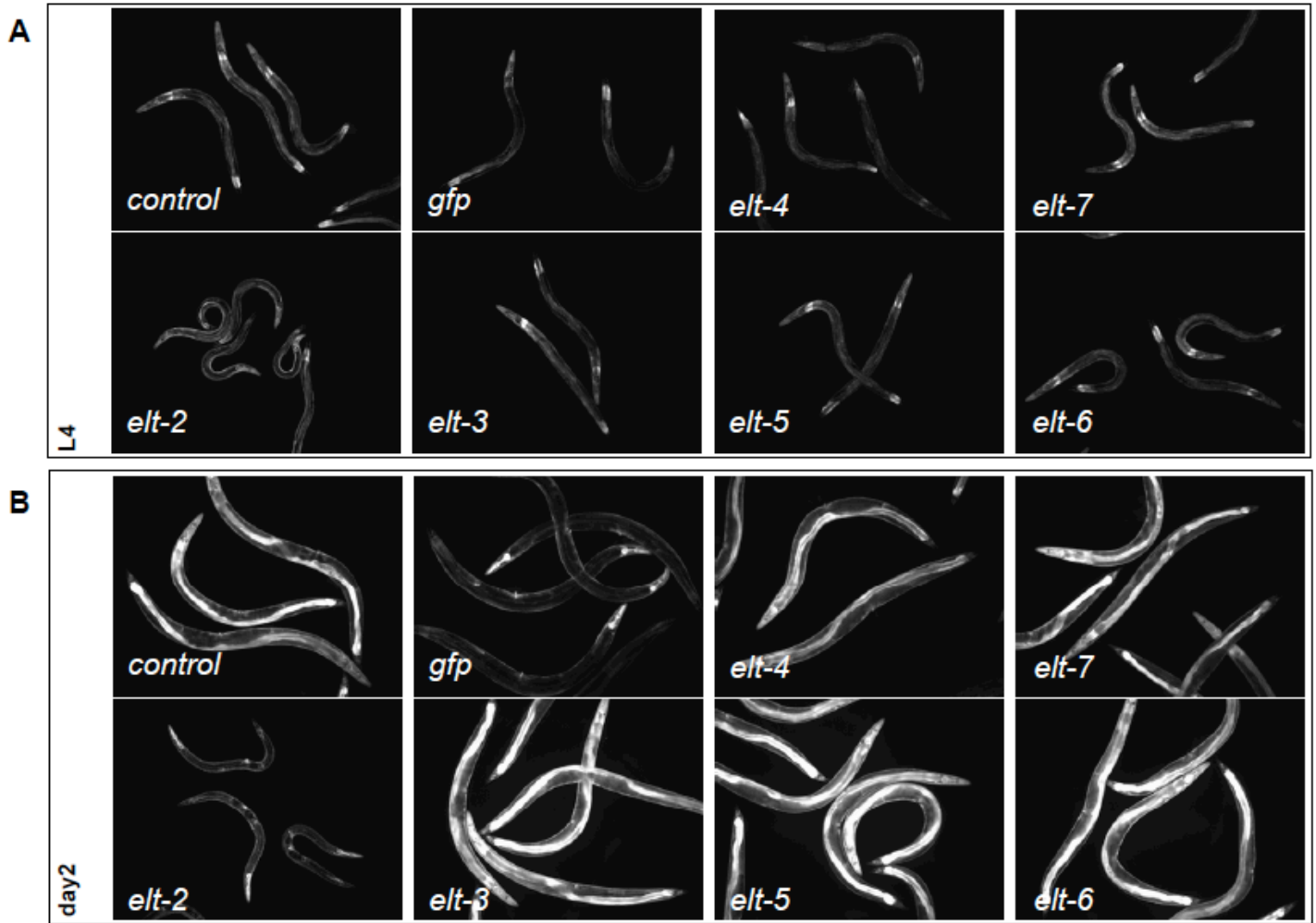


Figure S14. Effect by RNAi of SWI/SNF complex components on *Pdaf-16d/f::gfp* expression.

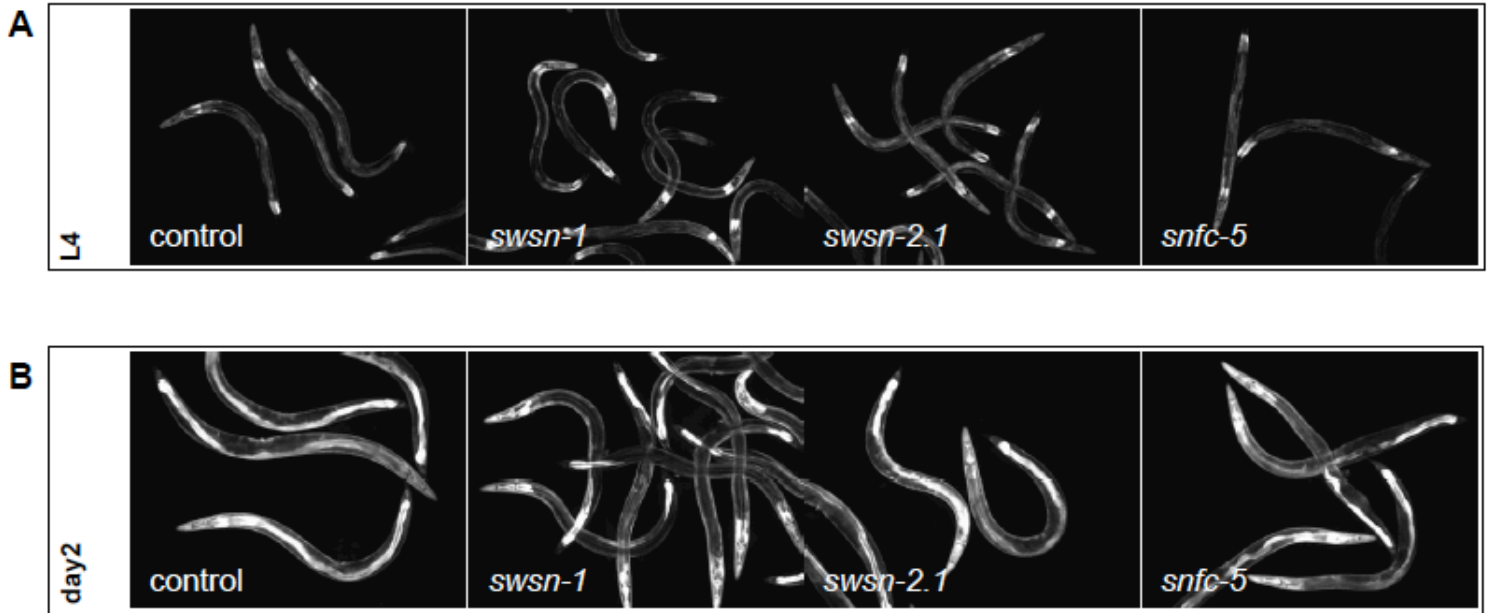


Figure S15: Lack of an effect of FUDR on lifespan.

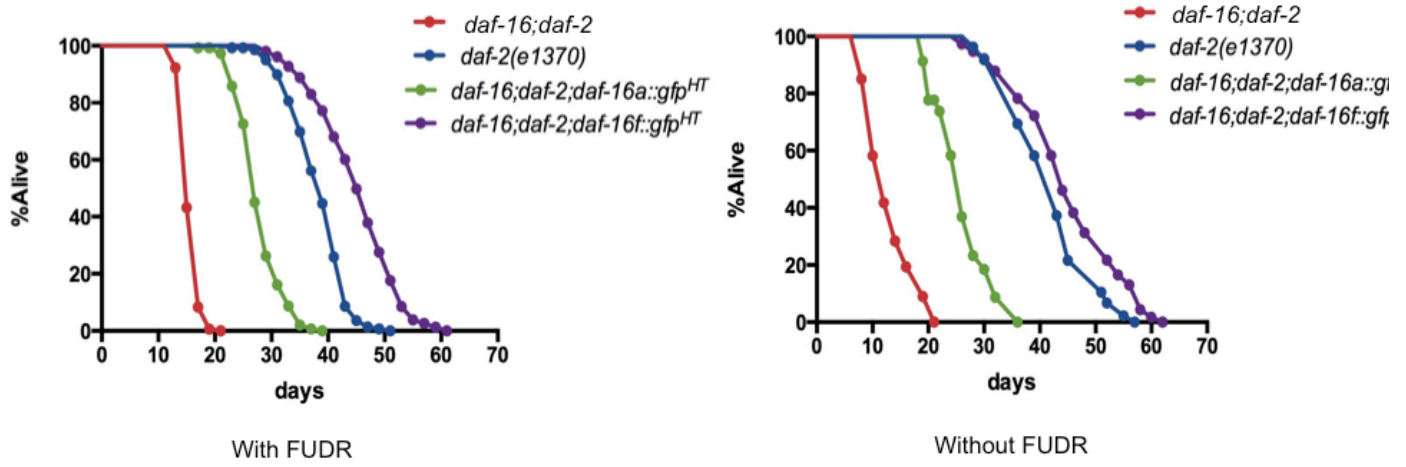


Table S1 : Analysis of the ESTs that correspond to *daf-16* isoforms

	# of cDNAs	Wormbase identity	Available cDNA sequences			note
			Clone/accession	5' EST	3' EST	
Unique to <i>daf-16f</i>	1	R13H8.f	KZ41_1781086	5		
Common to <i>daf-16f</i> and d:	2	R13H8.f/d	yk1377b02	5	3	
			yk359c8	5	3	
Unique to <i>daf-16a</i> (a1 and a2 isoforms are reported together):	11	R13H8.b/c	OSTF020B8_1	5		a1 = R13H8.b
			OSTF020D8_1	5		a1 = R13H8.b
			yk1204c09	5	3	a1 = R13H8.b
			yk1008b03	5	3	a1 = R13H8.b
			AF020343			mRNA a1 = R13H8.b
			IST_WI5_47437	5		a2 = R13H8.c
			yk31f10	5	3	a2 = R13H8.c
			AF020342			mRNA a2 = R13H8.c
			yk1337d04	5	3	a1/a2 = R13H8.b/c
			yk1006c10	5	3	a1/a2 = R13H8.b/c
			yk13f11	5	3	a1/a2 = R13H8.b/c
Common to <i>daf-16f</i>, d and a:	5	R13H8.f/d/b/c	yk350a5	5		
			yk1598c08	5	3	
			KZ41_1785504	5	3	
			yk1564b12	5	3	
			yk1556f11	5	3	
Unique to <i>daf-16b</i>:	6	R13H8.a	yk572a12	5		
			yk632g3	5		
			OSTF020E10_1	5		
			yk294b10	5		
			yk274c4	5	3	
			AF020344			mRNA
			OSTR020E10_1	3		
			OSTR020D8_1	3		
			OSTR020B8_1	3		
			yk14d11	3		
			yk178c8	5		
			yk1019c02	5	3	
			yk1196f06	5	3	
			yk1044b11	5	3	
			yk1048e05	5	3	
			yk32f8	5	3	
Unnamed isoform	1	R13H8.g	yk1160e04	5	3	

Table S2. Comparative level of *daf-16* isoform transcript

Comparative level of <i>daf-16</i> isoform transcript			
Genotype	<i>daf-16a</i>	<i>daf-16f</i>	generated from^{ref}
<i>daf-2(e1370)</i>	1 (control)	1 (control)	
<i>daf-16(mgDf50);daf-2(e1370)</i>	N. D.	N. D.	
<i>daf-16(mgDf50);daf-2(e1370);daf-16a::gfp^{HT}</i>	1.67 ± 0.17	N. D.	In this study
<i>daf-16(mgDf50);daf-2(e1370);daf-16a::gfp^{CF}</i>	10.19 ± 0.16	N. D.	Lin et al. [7]
<i>daf-16(mgDf50);daf-2(e1370);daf-16a::gfp^{TJ}</i>	22.95 ± 1.63	N. D.	Hederson et al. [8]
<i>daf-16(mgDf50);daf-2(e1370);daf-16a::gfp^{GR}</i>	432.85 ± 29.44	N. D.	Padmanabhan et al. [9]
<i>daf-16(mgDf50);daf-2(e1370);daf-16d/f::gfp^{HT}</i>	N. D.	4.57 ± 1.11	Kwon et al. [2]

N. D., not detected

Table S3. Lifespan analysis of *daf-16* isoform transgenic strains

Lifespan analysis of <i>daf-16</i> isoform transgenic strains				
Background	<i>daf-16</i> isoform	Mean LS \pm SEM (days)	Number of worms	P value vs control
exp.1^a				
N2	<i>daf-16</i> ⁺ (WT)	21.1 \pm 0.4	59	control
<i>daf-16(mgDf50)</i>	Null	15.0 \pm 0.1	144	< 0.0001
	<i>daf-16a::gfp</i> ^{HT}	19.4 \pm 0.3	103	0.0007
	<i>daf-16a::gfp</i> ^{CF}	23.3 \pm 0.3	126	< 0.0001
	<i>daf-16a::gfp</i> ^{TJ}	22.2 \pm 0.3	118	0.0215
	<i>daf-16a::gfp</i> ^{GR}	27.5 \pm 0.2	131	< 0.0001
	<i>daf-16d/f::gfp</i> ^{HT}	20.9 \pm 0.4	58	0.7682
<i>daf-2(e1370)</i>	<i>daf-16</i> ⁺ (WT)	38.5 \pm 0.4	139	control
<i>daf-16(mgDf50); daf-2(e1370)</i>	Null	15.9 \pm 0.1	155	< 0.0001
	<i>daf-16a::gfp</i> ^{HT}	28.1 \pm 0.3	149	< 0.0001
	<i>daf-16a::gfp</i> ^{CF}	40.9 \pm 0.4	155	< 0.0001
	<i>daf-16a::gfp</i> ^{TJ}	41.0 \pm 0.4	157	< 0.0001
	<i>daf-16a::gfp</i> ^{GR}	27.8 \pm 0.3	136	< 0.0001
	<i>daf-16d/f::gfp</i> ^{HT}	45.3 \pm 0.6	153	< 0.0001
exp.2				
N2	<i>daf-16</i> ⁺ (WT)	18.6 \pm 0.3	114	control
<i>daf-16(mgDf50)</i>	Null	13.6 \pm 0.2	137	< 0.0001
	<i>daf-16a::gfp</i> ^{HT}	17.3 \pm 0.3	56	0.0006
	<i>daf-16a::gfp</i> ^{CF}	23.6 \pm 0.3	127	< 0.0001
	<i>daf-16a::gfp</i> ^{TJ}	22.2 \pm 0.3	114	< 0.0001
	<i>daf-16a::gfp</i> ^{GR}	27.8 \pm 0.3	149	< 0.0001
	<i>daf-16d/f::gfp</i> ^{HT}	19.4 \pm 0.5	59	0.029
<i>daf-2(e1370)</i>	<i>daf-16</i> ⁺ (WT)	38.1 \pm 0.5	111	control
<i>daf-16(mgDf50); daf-2(e1370)</i>	Null	15.2 \pm 0.1	141	< 0.0001
	<i>daf-16a::gfp</i> ^{HT}	26.5 \pm 0.3	141	< 0.0001
	<i>daf-16a::gfp</i> ^{CF}	43.2 \pm 0.4	161	< 0.0001
	<i>daf-16a::gfp</i> ^{TJ}	39.2 \pm 0.4	154	0.1965
	<i>daf-16a::gfp</i> ^{GR}	26.6 \pm 0.3	130	< 0.0001
	<i>daf-16d/f::gfp</i> ^{HT}	44.9 \pm 0.5	176	< 0.0001
exp.3				
N2	<i>daf-16</i> ⁺ (WT)	19.9 \pm 0.3	128	control
<i>daf-16(mgDf50)</i>	Null	15.4 \pm 0.1	153	< 0.0001
	<i>daf-16a::gfp</i> ^{HT}	18.8 \pm 0.2	238	< 0.0001
	<i>daf-16a::gfp</i> ^{CF}	19.8 \pm 0.2	175	0.4561
	<i>daf-16a::gfp</i> ^{TJ}	21.3 \pm 0.3	127	< 0.0001
	<i>daf-16a::gfp</i> ^{GR}	26.3 \pm 0.2	151	< 0.0001
	<i>daf-16d/f::gfp</i> ^{HT}	20.2 \pm 0.3	165	0.0809
<i>daf-2(e1370)</i>	<i>daf-16</i> ⁺ (WT)	38.6 \pm 0.5	163	control
<i>daf-16(mgDf50);</i>	Null	16.1 \pm 0.1	187	< 0.0001

<i>daf-2(e1370)</i>	<i>daf-16a::gfp^{HT}</i>	31.9 ± 0.3	169	< 0.0001
	<i>daf-16a::gfp^{CF}</i>	33.5 ± 0.3	177	< 0.0001
	<i>daf-16a::gfp^{TJ}</i>	36.1 ± 0.3	180	< 0.0001
	<i>daf-16a::gfp^{GR}</i>	28.9 ± 0.3	203	< 0.0001
	<i>daf-16d/f::gfp^{HT}</i>	42.6 ± 0.5	191	< 0.0001

LS= lifespan; ^a indicates experiment depicted in Figure 2B and 2C.

Table S3. Lifespan analysis of *daf-16* isoform transgenic strains (continued)

Table S4. Lifespan analysis of *daf-16* isoform transgenic strains

Lifespan analysis of <i>daf-16</i> isoform transgenic strains				
Background	<i>daf-16</i> isoform	Mean LS \pm SEM (days)	Number of worms	P value vs control
exp.1				
<i>daf-2(e1368)</i>	<i>daf-16⁺(WT)</i>	33.6 \pm 0.8	67	control
<i>daf-16(mgDf50); daf-2(e1368)</i>	Null	15.0 \pm 0.2	75	< 0.0001
	<i>daf-16a::gfp^{HT}</i>	25.3 \pm 0.4	91	< 0.0001
	<i>daf-16d/f::gfp^{HT}</i>	27.7 \pm 0.4	102	< 0.0001
exp.2				
<i>daf-2(e1368)</i>	<i>daf-16⁺(WT)</i>	33.6 \pm 0.7	104	control
<i>daf-16(mgDf50); daf-2(e1368)</i>	Null	13.3 \pm 0.2	89	< 0.0001
	<i>daf-16a::gfp^{HT}</i>	22.2 \pm 0.4	74	< 0.0001
	<i>daf-16d/f::gfp^{HT}</i>	27.7 \pm 0.5	83	< 0.0001
exp.3^a				
<i>daf-2(e1368)</i>	<i>daf-16⁺(WT)</i>	29.8 \pm 0.4	101	control
<i>daf-16(mgDf50); daf-2(e1368)</i>	Null	15.5 \pm 0.2	100	< 0.0001
	<i>daf-16a::gfp^{HT}</i>	22.2 \pm 0.2	195	< 0.0001
	<i>daf-16d/f::gfp^{HT}</i>	27.3 \pm 0.3	215	< 0.0001

LS, lifespan

^a indicates experiment depicted in Figure 2D.

Table S5. Lifespan analysis of serially diluted *daf-16* RNAi

Lifespan analysis of serially diluted <i>daf-16</i> RNAi				
Background	RNAi^(dilution)	Mean LS ± SEM (days)	Number of worms	P value vs control
exp.1^a				
<i>daf-16(mgDf50); daf-2(e1370)</i>	control	14.0 ± 0.2	151	control
	<i>daf-16</i>	14.4 ± 0.2	172	0.0875
<i>daf-16(mgDf50); daf-2(e1370); daf-16d/f::gfp</i>	control	41.8 ± 0.4	288	control
	<i>daf-16</i>	17.6 ± 0.2	226	< 0.0001
	<i>daf-16^{(1/1)*}</i>	17.3 ± 0.2	171	< 0.0001
	<i>daf-16^{(1/4)*}</i>	21.9 ± 0.4	242	< 0.0001
	<i>daf-16^{(1/8)*}</i>	26.4 ± 0.4	257	< 0.0001
	<i>daf-16^{(1/16)*}</i>	30.4 ± 0.3	226	< 0.0001
	<i>daf-16^{(1/32)*}</i>	34.2 ± 0.4	264	< 0.0001
<i>daf-16^{(1/64)*}</i>	38.5 ± 0.4	255	< 0.0001	
exp.2				
<i>daf-16(mgDf50); daf-2(e1370)</i>	control	14.1 ± 0.1	131	control
	<i>daf-16</i>	14.3 ± 0.1	148	0.2444
<i>daf-16(mgDf50); daf-2(e1370); daf-16f::gfp</i>	control	54.1 ± 0.5	156	control
	<i>daf-16</i>	17.0 ± 0.3	77	< 0.0001
	<i>daf-16^{(1/1)*}</i>	16.8 ± 0.2	109	< 0.0001
	<i>daf-16^{(1/2)*}</i>	17.3 ± 0.3	104	< 0.0001
	<i>daf-16^{(1/4)*}</i>	18.4 ± 0.3	102	< 0.0001
	<i>daf-16^{(1/8)*}</i>	19.6 ± 0.4	117	< 0.0001
<i>daf-16^{(1/16)*}</i>	27.0 ± 0.8	91	< 0.0001	

() indicates dilution rate; (*daf-16* RNAi/*daf-16* RNAi + control RNAi)

* indicates temporal treatment of *daf-16* RNAi.

^a indicates experiment depicted in Figure 3F.

LS, lifespan

Table S7. Primer sequences used in this study

Primer sequences used in this study			
Primer name	Gene amplified	Used for	SEQUENCE (5'-3')
8.1cspf5qRT	<i>daf-16a</i>	Q-RT PCR	CACCGGATGATGTGATGATG
8.1cspf3qRT	<i>daf-16a</i>	Q-RT PCR	CTCCCGTATAGGTCAGCATC
8.1aspf5qRT	<i>daf-16b</i>	Q-RT PCR	CCTATTCGGATATCATTGCC
8.1aspf3qRT	<i>daf-16b</i>	Q-RT PCR	GGATCGAGTTCTTCCATCCG
8.1dspf5qRT	<i>daf-16d/f</i>	Q-RT PCR	CAATCTCGACCTCCATCAAC
8.1dspf3qRT	<i>daf-16d/f</i>	Q-RT PCR	CCCGTATAGGCTAGTTCTTC
8.1ORFcom5	<i>total daf-16</i>	Q-RT PCR	AAGCCGATTAAGACGGAACC
8.1ORFcom3	<i>total daf-16</i>	Q-RT PCR	GTAGTGGCATTGGCTTGAAG
acts-5	<i>Actin</i>	Q-RT PCR	CTCTTGCCCCATCAACCATG
acts-3	<i>Actin</i>	Q-RT PCR	CTTGCTTGAGATCCACATC
elt-2 RT fw2	<i>elt-2</i>	Q-RT PCR	GGGTTGATGATGGTTCCAAAC
elt-2 RT rv2	<i>elt-2</i>	Q-RT PCR	TTTCATCATCCTGAACTGGC
psa-1 RT fw1	<i>swn-1</i>	Q-RT PCR	GAAGTGCCGAAAGGAAAGGAA
psa-1 RT rv1	<i>swn-1</i>	Q-RT PCR	TTTCCTTCGGCGAGTTGTGG
Pdaf-16df5	<i>daf-16d/f</i>	Translational gfp fusion	TATTGCATGCCGTAGCTTAAAG
Pdaf16df3 BamHI	<i>daf-16d/f</i>	Translational gfp fusion	TCCGGGATCCGGCCTTGCCGGTT
Pdaf16bc5 Sall	<i>daf-16a</i>	Translational gfp fusion	CATTGTGACGCGCGCCCATG
Pdaf16bc3 BamHI	<i>daf-16a</i>	Translational gfp fusion	TTCGGGATCCTCAGCCAAAGACG AC
16D RNAi5	<i>daf-16d/f</i>	RNAi cloning	AACTGAAGCTTGATTCGCCGCTA C
16D RNAi3	<i>daf-16d/f</i>	RNAi cloning	CCCGTGCTAGCTAGTTCTTCCGC
DAF16 INT UP	<i>daf-16</i>	detecting deletion	CAATGAGCAATGTGGACAGC
DAF16 INT down	<i>daf-16</i>	detecting deletion	CCGTCTGGTCGTTGTCTTTT

Table S8. List of Strains used in this study

Strain Name	Genotype	Reference
	Wild type bristol	
CB1370	<i>daf-2(e1370)</i>	Kenyon et al. 1993
GR1307	<i>daf-16(mgDf50)</i>	Ogg et al. 1997
HT1890	<i>daf-16(mgDf50); daf-2(e1370)</i>	
HT2001	<i>daf-16(mgDf50);unc-119(ed3); daf16a1::GFP unc-119[LpIs24]</i>	Kwon et al. 2010
CF1407	<i>daf-16(mgDf50);muIs71 [pKL99(daf-16Ap::GFP::daf-16A(bKO)) + pRF4(rol-6)]</i>	Lin et al. 2001
TJ356	<i>daf-16(mgDf50); zIs356</i>	Henderson et al. 2001
RX 86	<i>daf-16a::gfp</i>	Padmanabhan et al. 2008
HT2058	<i>daf-16(mgDf50); daf-2(e1370); unc-119(ed3); daf16a1::a::GFP unc-119[LpIs24]</i>	This manuscript
HT2025	<i>daf-16(mgDf50);daf-2(e1370);muIs71 [pKL99(daf-16Ap::GFP::daf-16A(bKO)) +pRF4(rol-6)]</i>	This manuscript
HT2022	<i>daf-16(mgDf50);daf-2(e1370); zIs356</i>	This manuscript
HT 2055	<i>daf-16; daf-2; daf-16a::gfp^{GR}</i>	This manuscript
DR1572	<i>daf-2(e1368)</i>	
HT2006	<i>daf-16(mgDf50);daf-2(e1368)</i>	This Manuscript
HT1970	<i>daf-16(mgDf50);unc-119(ed3); daf-16d/f::GFP unc-119[LpIs14]</i>	Kwon et al. 2010
HT1883	<i>daf-16(mgDf50);daf-2(e1370);unc-119(ed3); daf-16d/f::GFP unc-119[LpIs14]</i>	Kwon et al. 2010
HT2014	<i>unc-119(ed3);Pdaf-16a::gfp unc-119[LpIs27]</i>	This manuscript
HT1992	<i>unc-119(ed3);Pdaf-16d/f::gfp unc-119[LpIs23]</i>	This manuscript
HT2063	<i>daf-16(mgDf50); daf-2(e1368); unc-119(ed3); daf16a1::a::GFP unc-119[LpIs24]</i>	This manuscript
HT2040	<i>daf-16(mgDf50); daf-2(e1368); unc-119(ed3); daf-16d/f::GFP unc-119[LpIs14]</i>	This manuscript